

ON-BOARD SYSTEM IDENTIFICATION OF SYSTEMS WITH UNKNOWN INPUT NONLINEARITY AND SYSTEM PARAMETERS

Song Liu

School of Mechanical Engineering
Purdue University
West Lafayette, IN47907
Email: liu1@ecn.purdue.edu

Bin Yao*

School of Mechanical Engineering
Purdue University
West Lafayette, IN47907
Email address: byao@ecn.purdue.edu

ABSTRACT

Input nonlinearities, or actuator nonlinearities, can be seen in a lot of systems and have significant effects on the system performance. From the controller design point of view, accurate yet simple model of input nonlinearities is essential to compensate their effects and to achieve high level control performance. Unfortunately, most input nonlinearities are neither known nor easy to characterize, especially when the input nonlinearities and unknown system parameters are present simultaneously in the system dynamics. Off-board calibration may be possible yet it is very time consuming and requires additional calibration systems.

This paper focuses on a class of systems with unknown input nonlinearities and system parameters and proposes an on-board system identification process to model the unknown nonlinearities. The input nonlinearities are decomposed into localized orthogonal basis and then estimated together with the system parameters. The proposed method is applied to model the nonlinear flow mapping of cartridge valves. Simulation and experimental results are obtained to illustrate the effectiveness and practicality of the proposed method.

INTRODUCTION

Input nonlinearities can be seen in a lot of systems, such as electrical motion control systems with nonlinear amplifiers, valve controlled electro-hydraulic systems, room temperature

control systems, chemical and biological processes, etc., and have significant effects on the system performance [1]. Some simple input/actuator nonlinearities, such as deadband, have been well addressed in many researches [1, 2]. When the input nonlinearities are known, they can be compensated by properly designed controllers, as the work done in [3, 4]. When the input nonlinearities are not exactly known but their structures are known, adaptive control technique can be applied to solve the problem, such as [1, 5]. In order to achieve precision control performance, the system control law must take into account the input nonlinearity and compensate it instead of neglecting or linearizing the input nonlinearity. Therefore it is essential to have an accurate yet simple model of the input nonlinearity for controller design purpose.

Most input nonlinearities are due to imperfect manufacturing processes or input devices' internal structures. There does not exist a common model or even common model structure for a same type of input devices. In a word, the input nonlinearity in mass produced systems is usually non-repeatable and has to be identified one by one. Though off-board calibration may be a solution, in addition to the need of a calibration system that increases cost, it is a very time consuming task, which is not suitable for industrial mass production.

This paper focuses on a class of nonlinear systems described in (1).

$$\dot{x} = \Phi^T(x) \cdot \theta + f(u, x) \quad (1)$$

* Address all correspondence to this author.

where x and u are the system state and input signal, respectively; $\varphi(x) = [\varphi_1(x), \varphi_2(x), \dots, \varphi_r(x)]^T$ is a set of known regressors, and $\theta = [\theta_1, \theta_2, \dots, \theta_r]^T$ is a set of unknown system parameters; $f(u, x)$ is the unknown input nonlinearity, which is a function of the input signal u as well as the system state x . An automated on-board identification algorithm to model the input nonlinearity, which utilize only the available system information, such as system output or state, is proposed in the paper.

Difficulties of on-board identification include:

- 1) Available information is very limited. Even though the system has full state feedback, there is usually no measurement of the value of the input nonlinearity $f(u, x)$ and the derivatives of the system states \dot{x} .
- 2) The system dynamics is also subject to parametric uncertainties. The presence of unknown system parameters makes the system identification even harder.
- 3) Experimental condition is very difficult to satisfied due to the inability to arbitrarily set system states.

In this paper, the unknown input nonlinearity and other unknown system parameters will be determined simultaneously from the system dynamics via certain intelligent integration of nonlinear function decomposition and on-line parameter estimation algorithms. Experimental conditions for accurate parameter estimations are carefully examined to obtain practical on-board tests that can run for accurate modelling of the input nonlinearity. The proposed technique is applied to model the nonlinear flow mapping of cartridge valves. Simulation and experimental results are presented to illustrate the effectiveness of the proposed method.

The objective of the proposed technique is to build a model of the input nonlinearity for the controller design purpose. The model obtained by the proposed technique is not necessary to be a 'perfect' model for analysis purpose. As long as the model is accurate enough in the important working range and improves control performance significantly, the objective is achieved.

PROBLEM FORMULATION

The following assumptions are made in this paper:

Assumption 1. *The system has full state feedback, hence u and x are known or measurable. However, the value of $f(u, x)$ and the derivative of the system state, i.e., \dot{x} , are not measurable.*

Assumption 2. *$f(u, x)$ is bounded though the value of $f(u, x)$ is not measurable.*

Assumption 3. *The system is controlled by a well designed controller and stable, therefore both x and u have bounded value, which implies that the unknown input nonlinearity $f(u, x)$ is practically defined on a compact set on $u - x$ surface.*

Assumption 4. *The system parameters θ are unknown but bounded with known bounds. The regressor $\varphi(x)$ is known.*

There are many ways to approximate an unknown function, such as the neural network [6], Fourier decomposition [7], Wavelet decomposition [8] and so on. The basic idea of all approximation methods is to decompose an unknown function into a set of basis functions with their own weighting factors, as shown in (2).

$$f(u, x) = \bar{f}(u, x) + \Delta, \quad \bar{f} = \varphi_f^T(u, x) \cdot \theta_f \quad (2)$$

where $\bar{f}(u, x)$ is the approximation of $f(u, x)$ and Δ represents the approximation or modelling error, $\varphi_f^T = [\varphi_{f1}, \varphi_{f2}, \dots, \varphi_{fn}]$ is a finite dimension vector of basis functions, and $\theta_f^T = [\theta_{f1}, \theta_{f2}, \dots, \theta_{fn}]$ is a vector of unknown parameters or weighting factors.

However, straightforward application of the above approximation seldom leads to satisfactory approximation due to the following practical limitation. Namely, to have a reasonably small approximation error Δ , a huge number of basis functions (i.e., large n) have to be used. This is especially true for the input nonlinearities having non-smooth components such as discontinuous frictions or deadband. Consequently, to obtain the approximation of the input nonlinearity $\bar{f}(u, x)$, huge number of parameters θ_f have to be adapted or estimated simultaneously from the limited experimental data sets, which makes it impossible to use the well-known parameter estimation algorithms having better converging properties due to the difficulty of running on-board experiments to satisfy the experimental conditions needed by those algorithms. For example, the least square estimation (LSE) algorithm needs the persistent excitation condition for parameter convergence, which, loosely speaking, can be satisfied only if rich enough data sets covering the entire working ranges of the control input u and the system state x are available. However, for on-board identification where the input component cannot be removed from the actual system, x is not an experimental variable that can be freely controlled and there is usually no way to conduct experiments that cover the entire range of $u - x$. Another problem is the Gibbs phenomena, i.e., when a discontinuous function is approximated by a finite number of basis functions, such as Fourier decomposition, severe oscillations exist around the discontinuous points.

If the input u and state x do not span the entire region, the nonlinearities that are not adequately exercised can not be observed in the experimental data, hence it is impossible to estimate the nonlinearities accurately in the inaccessible area. However, from controller design point of view, the inaccessible area are trivial because if a well designed experiment can not access the

area the closed loop system is unlikely to operate in the area. Instead of a global model for the unknown nonlinearity, only local properties on the area where the system operates are essential to improve control performance and therefore the main concern of the paper. The paper uses localized basis functions to bypass the problems associated with the global basis functions.

Substituting (2) into (1), one can obtain:

$$\dot{x} = \Phi^T(x) \cdot \theta + \Phi_f^T(u, x) \cdot \theta_f + \Delta \quad (3)$$

Defining $\Phi_{new}^T = [\Phi(x)^T, \Phi_f(u, x)^T]$ and $\theta_{new}^T = [\theta^T, \theta_f^T]$, (3) can be written in a compact form as

$$y = \Phi_{new}^T \cdot \theta_{new} + \Delta \quad (4)$$

(4) is in the standard linear regression form with respect to the unknown parameters θ_{new} with $y = \dot{x}$ being the model output and Δ as the model error. Thus, the original problem of automated on-board modelling of input nonlinearities in the presence of unknown system parameters is transformed into the tractable problem of accurate parameter estimation based on the linear regression model (4). The rest of the paper thus focuses on the selection of suitable basis functions $\Phi_f(u, x)$, the design of experiments, and the use of the least square algorithm (LSE) to minimize the effect of model error Δ for accurate parameter estimation.

IDENTIFICATION OF INPUT NONLINEARITIES

Based on Assumption 3, the input nonlinearity is practically defined on a compact support on $u-x$ surface. It is reasonable to cut the support on $u-x$ surface into small blocks, where u_{Nu} and x_{Nx} represent the maximal values of u and x respectively. Each block is named after the indices of u and x , e.g. I_{ij} , as shown in Fig. 1. The distances between u_i and u_{i+1} or x_j and x_{j+1} do not have to be equally spaced. As the function approximation will be done on each small block instead of on the entire region, *a priori* knowledge about the input nonlinearity can be used to help choose the spacing to have a reasonable good model approximation accuracy while minimizing the number of blocks needed. For example, if it is known that the deadband may happen around some input value though the exact value is not known, relatively small spacing should be used in the region near that input value. On the other hand, at the region where one knows the input nonlinearity may not change drastically, relatively larger spacings can be used to reduce the computation load.

On each small block I_{ij} , it is assumed that the value of the input nonlinearity does not change drastically and thus the input nonlinearity can be approximated as a Taylor series with respect

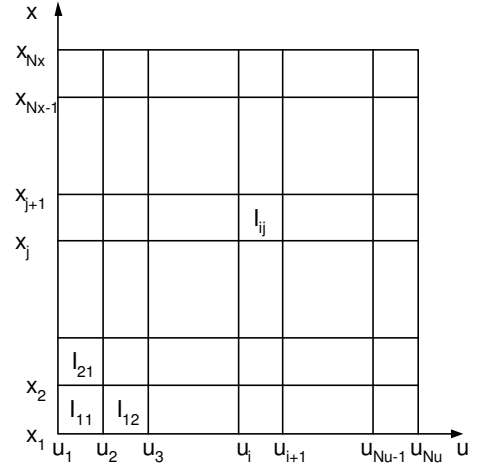


Figure 1. Cutting the $u-x$ surface into small blocks.

to the nominal point :

$$f(u, x)|_{(u, x) \in I_{ij}} = f(\bar{u}_i, \bar{x}_j) + \frac{\partial f}{\partial u}|_{(\bar{u}_i, \bar{x}_j)} \tilde{u} + \frac{\partial f}{\partial x}|_{(\bar{u}_i, \bar{x}_j)} \tilde{x} + \frac{1}{2} \frac{\partial^2 f}{\partial u^2}|_{(\bar{u}_i, \bar{x}_j)} \tilde{u}^2 + \frac{1}{2} \frac{\partial^2 f}{\partial x^2}|_{(\bar{u}_i, \bar{x}_j)} \tilde{x}^2 + \frac{1}{2} \frac{\partial^2 f}{\partial u \partial x}|_{(\bar{u}_i, \bar{x}_j)} \tilde{u} \tilde{x} + \Delta \quad (5)$$

where (\bar{u}_i, \bar{x}_j) represents the nominal working point in the block of I_{ij} , $\tilde{u} = u - \bar{u}_i$ and $\tilde{x} = x - \bar{x}_j$, and Δ represents all higher order terms and modelling error. *A priori* knowledge about the input nonlinearity as well as the required model approximation accuracy can be used to determine how many terms to keep. For simplicity, in this paper, all terms up to second order are kept while all higher order terms are considered as modelling error. The input nonlinearity in the block of I_{ij} is therefore approximated by a model given by

$$\bar{f}(u, x)|_{(u, x) \in I_{ij}} = \Phi_{ij}^T \cdot \theta_{ij} \quad (6)$$

where $\Phi_{ij}^T = \begin{cases} [1, \tilde{u}, \tilde{x}, \tilde{u}^2, \tilde{x}^2, \tilde{u}\tilde{x}] & (u, x) \in I_{ij}, \\ [0, 0, 0, 0, 0, 0] & \text{otherwise.} \end{cases}$ and $\theta_{ij}^T = [f(u, x), \frac{\partial f}{\partial u}, \frac{\partial f}{\partial x}, \frac{\partial^2 f}{\partial u^2}, \frac{\partial^2 f}{\partial x^2}, \frac{\partial^2 f}{\partial u \partial x}]|_{(\bar{u}_i, \bar{x}_j)} \in \mathbb{R}^6$.

With the above local approximations, on the entire region, the approximated input nonlinearity is:

$$\bar{f}(u, x) = \sum_{j=1}^{N_x} \sum_{i=1}^{N_u} \Phi_{ij}^T \cdot \theta_{ij} \quad (7)$$

which is in the form of (2) with $\Phi_f^T = [\Phi_{11}^T, \Phi_{12}^T, \dots, \Phi_{1N_x}^T, \Phi_{21}^T, \dots, \Phi_{i,j}^T, \dots, \Phi_{N_u N_x}^T]$, $\theta_f^T = [\theta_{11}^T, \theta_{12}^T, \dots, \theta_{1N_x}^T, \theta_{21}^T, \dots, \theta_{i,j}^T, \dots, \theta_{N_u N_x}^T]$. However,

different from (2), the basis functions ϕ_{ij} in (7) are localized, which enables the accurate parameter estimations to be carried out for individual blocks where sufficient data exist and the condition for applying the LSE algorithm is satisfied. Those regions normally correspond to the actual working ranges that the system is likely to operate, and thus precise modelling of the input nonlinearity in those regions are important for good control performance as well.

Regroup the experimental data according to the blocks they belong to. For simplicity, assume that $\{u(k), x(k), \bar{f}(k), k = 1, 2, \dots, N_{ij}\}$ are the set of experimental data falling into the block I_{ij} , i.e., $(u(k), x(k)) \in I_{ij}, \forall k = 1, 2, \dots, N_{ij}$ where N_{ij} represents the number of points. From (6), a matrix form can be obtained for the block I_{ij} :

$$[\bar{f}(u, x)]|_{(u, x) \in I_{ij}} = \Phi_{ij} \cdot \theta_{ij} + [\Delta] \quad (8)$$

where $[\bar{f}(u, x)]|_{(u, x) \in I_{ij}}$ represents the vector of the value of the input nonlinearities and $\Phi_{ij} = [\phi_{ij}(1), \phi_{ij}(2), \dots, \phi_{ij}(N_{ij})]^T$. If $\Phi_{ij}^T \Phi_{ij}$ is invertible – a condition that can be satisfied relatively easily due to the small number of parameters to be estimated, then, the experimental data are rich enough to give a good LSE estimate of θ_{ij} on the block I_{ij} :

$$\hat{\theta}_{ij} = (\Phi_{ij}^T \Phi_{ij})^{-1} \Phi_{ij}^T \cdot [\bar{f}(u, x)]|_{(u, x) \in I_{ij}} \quad (9)$$

In practice, one can check the condition number of $\Phi_{ij}^T \Phi_{ij}$ instead of its invertibility to make sure the above estimation is numerically well-conditioned for reliable estimations.

For the blocks where $\Phi_{ij}^T \Phi_{ij}$ is not invertible or ill-conditioned, it is impossible to have an accurate estimate of θ_{ij} as the experimental data obtained do not provide enough information on I_{ij} . Therefore one should not force the system to estimate θ_{ij} . The nonlinearities in these regions should be obtained via other means such as the extrapolation based on the model obtained for the blocks where rich data are available.

If the value of the input nonlinearity is known or measurable, (8) is ready for LSE algorithm. However, as discussed in the previous section, the actual value of the input nonlinearity is practically not measured in on-board experiments, the input nonlinearity must be identified with the unknown system parameters simultaneously. With ϕ_{new} and θ_{new} in (4) defined as $\phi_{new}^T = [\phi^T, \phi_{11}^T, \phi_{12}^T, \dots, \phi_{1N_x}^T, \phi_{21}^T, \dots, \phi_{ij}^T, \dots, \phi_{N_u N_x}^T]$ and $\theta_{new}^T = [\theta^T, \theta_{11}^T, \theta_{12}^T, \dots, \theta_{1N_x}^T, \theta_{21}^T, \dots, \theta_{ij}^T, \dots, \theta_{N_u N_x}^T]$, the LSE algorithm can be used to obtain the estimates of θ and θ_{ij} simultaneously for the blocks where the local persistent excitation condition is satisfied.

In practice, although x is measurable, \dot{x} may not be measurable. The well known low-pass filtering technique in the indirect

adaptive control, such as self tuning regulator, can be applied here to solve the problem [9]. In order to make (4) implementable for parameter estimation algorithms, a low pass filter, such as the one in (10), can be applied to the regressor ϕ_{new} as well as the virtual output \dot{x} .

$$H_f(s) = \frac{\omega_n^2}{s^2 + 2\zeta\omega_n s + \omega_n^2} \quad (10)$$

where ζ and ω_n are the damping ratio and natural frequency of the low pass filter respectively. Applying the linear filter (10) to both sides of Eq. (4) leads to:

$$\dot{x}_f = \phi_{newf}^T \cdot \theta_{new} + \Delta_f \quad (11)$$

where \dot{x}_f , ϕ_{newf}^T and Δ_f represent the filtered \dot{x} , ϕ_{new} and Δ . (11) is ready to implement to obtain estimates of θ and θ_{ij} simultaneously for the blocks where the local persistent excitation condition is satisfied.

The above method is to pass the signal through a discontinuous rectangular window defined on each block I_{ij} , which would usually results in discontinuous estimation of which discontinuity happens at the block boundaries. To avoid these discontinuity artifacts, it is necessary to use smooth windows [8]. The lapped projectors, which split signal in orthogonal components with overlapping supports [8], will be used to smooth the discontinuous estimation.

For simplicity, two orthogonal projectors that decompose any $f \in L^2(\mathbb{R})$ in two orthogonal components $P^+ f$ and $P^- f$ whose supports are $[-1, +\infty)$ and $(-\infty, 1]$ respectively are constructed for demonstration.

$$\begin{aligned} P^+ f(t) &= \beta(t)[\beta(t)f(t) + \beta(-t)f(-t)] \\ P^- f(t) &= \beta(-t)[\beta(-t)f(t) - \beta(t)f(-t)] \end{aligned} \quad (12)$$

where $\beta(t)$ is a monotone increasing profile function, such as
$$\beta(t) = \begin{cases} 0 & \text{if } t < -1 \\ 1 & \text{if } t > 1 \end{cases} \text{ and } \beta^2(t) + \beta^2(-t) = 1 \quad \forall t \in [-1, 1].$$

Theorem 1. (Coifman and Meyer) *The operators P^+ and P^- are orthogonal projectors respectively on W^+ and W^- . The spaces W^+ and W^- are orthogonal and $P^+ + P^- = \text{Identity}$.*

The proof of the theorem can be seen in [8]. The projectors can be easily shifted to $[a - \eta, +\infty)$ and $(-\infty, a + \eta]$ or repeated at different locations to perform a signal decomposition into orthogonal pieces whose supports overlap. It is also straight forward to extend the projectors from one-dimensional to two-dimensional. There exist several well known lapped orthogonal bases, such as the family of local cosine functions [8].

AUTOMATED MODELLING OF CARTRIDGE VALVE FLOW MAPPING

The proposed technique is applied to identify and model the nonlinear flow mapping of proportional poppet-type cartridge valves. Proportional poppet-type cartridge valves are the key elements of the energy saving programmable valves, shown in Fig. 2, which have been shown in our previous studies to be able to achieve excellent motion control performance while significantly saving energy usage. Unlike costly conventional four-way valves, the cartridge valve has simple structure and is easy to manufacture, but its complicated mathematical model makes the controller design and implementation rather difficult. Our previous works used either an off-line individually calibrated or manufacturer supplied flow mappings as the model of the cartridge valves. Neither method is ideal for industrial wide applications as the former method is time-consuming and needs trained engineers with additional flow sensors while the later leads to significantly degraded control performance due to the inaccuracy of the manufacturer supplied flow mappings.

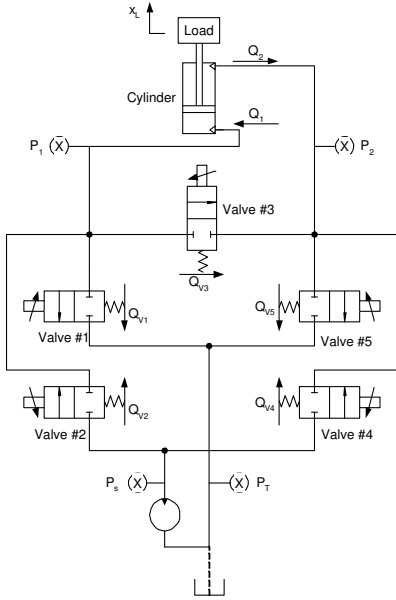


Figure 2. Energy Saving Programmable Valves.

Neglecting cylinder leakages, the cylinder pressure dynamics can be written as [10]:

$$\frac{V(x)}{\beta_e} \dot{P} = -A\dot{x} + Q(u, \Delta P) \quad (13)$$

where $V(x)$ is the total cylinder volume including connecting hose, x is the displacement of the cylinder rod, β_e is the effective

bulk modulus, P represents the cylinder pressure, A is the cylinder ram area, Q is the metered flow rate, u is the input signal to the valve, and ΔP is the pressure drop across the valve. In (13), A is a known parameter, u is control signal sent out by the controller, x , P , ΔP are measurable, and $V(x)$ is calculable. The effective bulk modulus β_e is usually an unknown parameter and changes significantly with working conditions.

Define $\theta_{\beta_e} = \frac{1}{\beta_e}$, and assume that the nonlinear flow rate $Q(u, \Delta P)$ is decomposed into the form given by (7), the cylinder pressure dynamics can then be re-written as:

$$A\dot{x} = -V(x)\dot{P} \cdot \theta_{\beta_e} + \sum_{j=1}^{N_x} \sum_{i=1}^{N_u} \phi_{ij}^T \cdot \theta_{ij} + \Delta \quad (14)$$

(14) fits the format of (3) and (4) with $A\dot{x}$ being the virtual model output and $\phi_{new}^T = [-V(x)\dot{P}, \phi_{11}^T, \phi_{12}^T, \dots, \phi_{1N_x}^T, \phi_{21}^T, \dots, \phi_{ij}^T, \dots, \phi_{N_u N_x}^T]$ and $\theta_{new}^T = [\theta_{\beta_e}, \theta_{11}^T, \theta_{12}^T, \dots, \theta_{1N_x}^T, \theta_{21}^T, \dots, \theta_{ij}^T, \dots, \theta_{N_u N_x}^T]$. Hence the proposed method can be applied to identify and model the nonlinear flow mapping $Q(u, \Delta P)$.

SIMULATIONS AND EXPERIMENTS

Simulations and experiments are done to illustrate the effectiveness of the proposed automated on-board modelling technique for input nonlinearities. In the simulation, a non-smooth two-dimensional nonlinear function is identified by the proposed method. Fig. 3 shows the simulation results, where the continuous curves represent the true value of the function while the 'X' represents the estimated values. Since *a priori* knowledge may provide information about where the deadband would occur, eg., between $u = 1$ and $u = 2$ in this simulation, relatively small spacing can be chosen in this region. And relatively large spacing can be set where the function does not change drastically.

In the experiments, the programmable valves are used to control the boom motion of a three degree-of-freedom hydraulic robot arm at the Ray W. Herrick Laboratories. The working mode selection and the coordinate controller design for the programmable valves can be found in [11]. For simplicity, the following study is concentrated on the automated modelling of the flow mapping for the valve #2 shown in Fig. 2 for the programmable valves. The boom motion is controlled to track a swiped sinusoidal reference trajectory, whose frequency varies from 0.1 Hz to 0.5 Hz over 80 seconds. Fig. 4 shows how the blocks are generated and where the obtained experimental data locate. The fine grids between 1 volt and 4 volts for the control input is for more accurate flow estimation to deal with the unknown deadband in this region.

It is obvious that the obtained on-board experiment data do not cover the entire region, and it is impossible to have flow estimates in the blocks which suffer low data or no data at all.

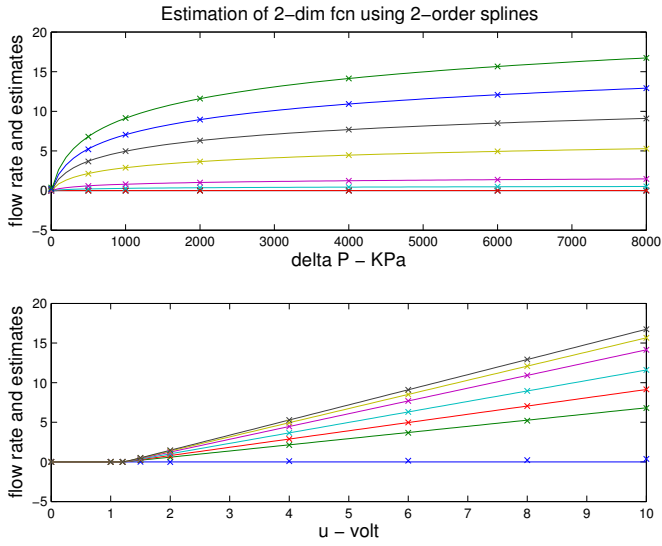


Figure 3. Estimation of a Two Dimensional Function.

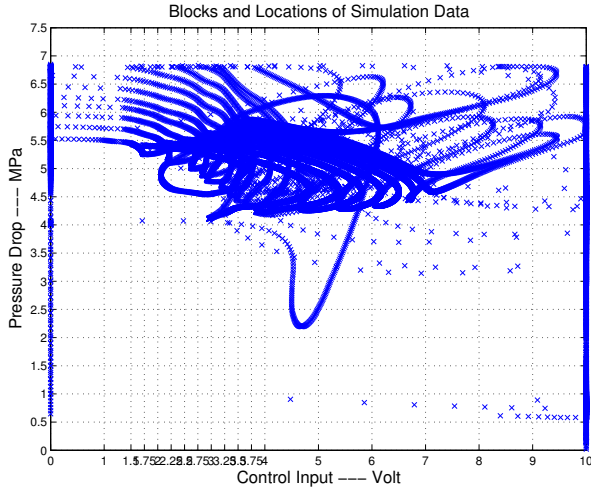


Figure 4. Blocking and Location of Experimental Data.

However, with the localized orthogonal basis functions and by checking the experimental condition on each block, one can easily control the estimation process with the proposed method. For example, by setting the threshold for the condition number as 1×10^8 and only estimating the flow mappings for blocks having the condition number less than the threshold, the estimated flow mapping with extrapolations is compared with the individually calibrated one as shown in Table 1. In Table 1, the flow rate has a unit of L/min , the upper number represents the value given by the estimated flow mapping with the proposed method and the lower number the value from individually calibrated one. It is seen that both values are quite close to each other, illustrating the

Table 1. Estimated Flow Mapping vs. True Value

	4v	5v	6v	7v
4.5MPa	7.33	12.02	17.79	22.96
	8.00	11.83	17.57	22.60
5MPa	8.20	12.44	17.37	22.62
	8.00	12.22	17.18	21.95
5.5MPa	7.98	12.02	NA	NA
	7.97	12.00	16.39	20.61

reasonable modelling accuracy of the proposed method.

In the above study, neither the valve control input u nor the pressure drop ΔP is arbitrarily controlled. This results in lack of data in a lot of regions. For more accurate flow mapping estimation, one can simplify the two-dimensional flow mapping into a series of one-dimensional mappings, i.e., fix the control input u and estimate a bunch of one-dimensional function described as follows:

$$Q(u, \Delta P)|_{u=u_i} = Q_i(\Delta P), \quad i = 1, 2, \dots, Nu \quad (15)$$

Figure 5 shows one of the experimentally estimated flow mappings with this method.

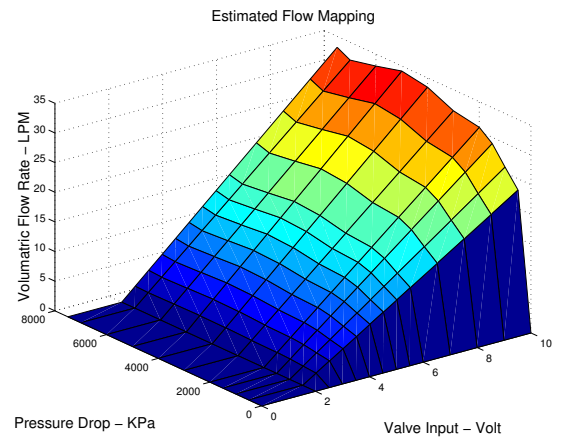


Figure 5. Estimated Cartridge Valve Flow Mapping.

To check the accuracy of the estimated flow mapping, the above estimated flow mappings along with the individually calibrated one in [11, 12] or the manufacture supplied one in [13] are used in the same Adaptive Robust Controller (ARC) to control the boom motion of the hydraulic arm respectively. Specifically,

the ARC controller design by Liu and Yao in [13] with the control gains set to 16 and adaptation turned off is used for all the experiments. The control task is a smooth point-to-point motion trajectory as shown in Fig. 6. The trajectory includes high acceleration and high speed tracking periods as well as constant positioning regulation periods, and reflects both of the two typical control problems — tracking control and positioning control. It is a very good evaluation to check the accuracy of the identified model. The tracking performances with different models are shown in the second plot of Fig. 6. Although the controller with the experimentally estimated flow mappings performs not as good as the one with individually calibrated flow mappings due to the limited on-board experimental data used in the flow mapping estimation, it does perform better than the one using the manufacturer supplied flow mappings.

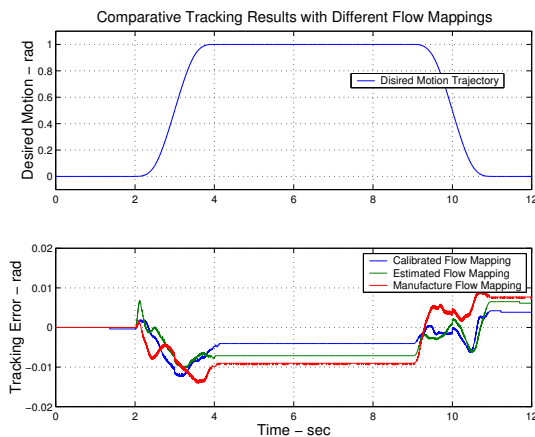


Figure 6. Comparative Tracking Results with Different Flow Mappings.

CONCLUSIONS

Accurate on-board identification of the input nonlinearity in the presence of unknown parameters is very important to improve system control performance. This paper proposes an approach to decompose the unknown input nonlinearity with some localized orthogonal basis functions. The weighting parameters of the basis functions as well as the unknown system parameters are then estimated simultaneously based on the system dynamics. Application of the proposed technique to identify and model the nonlinear flow mappings of proportional cartridge valves demonstrates the feasibility of the proposed method.

ACKNOWLEDGEMENT

The work is supported in part through the National Science Foundation under the grant CMS-0220179.

REFERENCES

- [1] Tao, G., and Kokotovic, P. V., 1996. *Adaptive Control of Systems with Actuator and Sensor Nonlinearities*. John Wiley & Sons, Inc.
- [2] Liu, S., and Yao, B., 2004. "Characterization and attenuation of sandwiched deadband problem using describing function analysis and its application to electro-hydraulic systems controlled by closed-center valves". In ASME International Mechanical Engineering Congress and Exposition. IMECE 2004-60946.
- [3] Fortgang, J. D., George, L. E., and Book, W. J., 2002. "Practical implementation of a dead zone inverse on a hydraulic wrist". In Proc. of ASME International Mechanical Engineering Congress and Exposition. IMECE 2002-39351.
- [4] Bu, F., and Yao, B., 2000. "Nonlinear adaptive robust control of hydraulic actuators regulated by proportional directional control valves with deadband and nonlinear flow gain coefficients". In Proc. of American Control Conference, pp. 4129–4133.
- [5] Taware, A., Tao, G., and Teolis, C., 2001. "An adaptive dead-zone inverse controller for systems with sandwiched dead-zones". In Proceedings of the American Control Conference, pp. 2456–2461.
- [6] Haykin, S., 1999. *Neural Networks, A Comprehensive Foundation*, 2nd ed. Pearson Education.
- [7] Oppenheim, A. V., and Schaffer, R. W., 1985. *Digital Signal Processing*. Prentice Hall, N.J.
- [8] Mallat, S., 1999. *A Wavelet Tour of Signal Processing*. Academic Press.
- [9] Karl J. Åström and Björn Wittenmark, 1995. *Adaptive Control*, 2nd edition ed. Addison-Wesley.
- [10] Merritt, H. E., 1967. *Hydraulic Control Systems*. John Wiley & Sons.
- [11] Liu, S., and Yao, B., 2003. "Coordinate control of energy-saving programmable valves". In ASME International Mechanical Engineering Congress and Exposition. IMECE 2003-42668.
- [12] Liu, S., and Yao, B., 2004. "Programmable valves: a solution to bypass deadband problem of electro-hydraulic systems". In Proc. of American Control Conference, pp. 4438–4443.
- [13] Liu, S., and Yao, B., 2004. "Adaptive robust control of programmable valves with manufacture supplied flow mapping only". In IEEE Conference on Decision and Control.